2020

Polyvinyl Alcohol Cryogel Based Vessel Mimicking Material for Modelling the Progression of Atherosclerosis

Andrew Malone
Technological University Dublin

Sean Cournane
St. Vincent's University Hospital, Dublin

Izabela Naydenova
Technological University Dublin, izabela.naydenova@tudublin.ie

Andrew J. Fagan
Mayo Clinic, Rochester

Jacinta Browne
Technological University Dublin, jacinta.browne@tudublin.ie

Recommended Citation

Malone, A., Cournane, S., Naydenova, I. et al (2020). Polyvinyl alcohol cryogel based vessel mimicking material for modelling the progression of atherosclerosis. *Physica Medica*, vol. 69, p.1-8. doi:10.1016/j.ejmp.2019.11.012

Physica Medica 69 (2020) 1–8

Contents lists available at ScienceDirect

Physica Medica

journal homepage: www.elsevier.com/locate/ejmp

Original paper

Polyvinyl alcohol cryogel based vessel mimicking material for modelling the progression of atherosclerosis

Andrew J. Malone[a,*], Sean Cournane[b], Izabela G. Naydenova[a], Andrew J. Fagan[c], Jacinta E. Browne[a,c]

[a] School of Physics and Clinical & Optometric Sciences, College of Science and Health, Technological University Dublin, Dublin, Ireland
[b] St. Vincent's University Hospital, Dublin, Ireland
[c] Department of Radiology, Mayo Clinic, Rochester, MN, USA

ARTICLE INFO

Keywords:
Mechanical characterisation
Doppler ultrasound
Flow phantom
Atherosclerosis

ABSTRACT

Purpose: The stiffness of Polyvinyl-alcohol cryogel can be adjusted through application of consecutive freeze-thaw cycles. This material has potential applications in the production of tissue mimicking phantoms in diagnostic ultrasound. The aim of this study was to use PVA-c to produce a range of geometrically and acoustically identical vessel phantoms modelling stages of atherosclerosis which could be verified through mechanical testing, thus allowing for more precision in quantitative in-vitro flow analysis of atherosclerosis.
Methods: A series of anatomically realistic walled renal artery flow phantoms were constructed using PVA-c. In order to ensure precise modelling of atherosclerosis, a modified procedure of ISO27:2017 was used to compare the mechanical properties of PVA-c. Results were compared for the standard "dumbbell" test object and a modified vessel test object. The geometric accuracy and reproducibility of the vessel models were tested before and after implantation in flow phantoms.
Results: No significant difference was found between the mechanical properties of the dumbbell test samples and the vessels for any number of freeze thaw cycles, with a correlation coefficient of $R^2 = 0.9767$ across the dataset, indicating that a direct comparison between the mechanical properties of the dumbbell test samples and the phantom vessels was established. The geometric reproducibility showed that before and after implantation there was no significant difference between individual vessel geometries ($p = 0.337$ & $p = 0.176$ respectively).
Conclusions: Polyvinyl-alcohol cryogel is a useful material for the production of arterial flow phantoms. Care should be taken when using this material to ensure its mechanical properties have been correctly characterised. The guidelines of ISO37:2017 potentially provide the best procedure to ensure this.

1. Introduction

Cardiovascular disease (CVD) is the leading cause of death in the world [1]. CVD is typically characterised by a number of biological processes, such as intimal thickening in the vessel wall, development of atherosclerotic plaque, and the stiffening of arterial walls. In addition, it has been found that a number of life limiting and life threatening conditions are correlated with the mechanical properties of arterial tissue [2–4]. There is a clinical interest in each of these features, of which this work explores the stiffening of artery walls primarily. Several methods are used for the diagnosis of CVD, including magnetic resonance angiography (MRA), computed tomography angiography (CTA), and Doppler ultrasound (US). These methods invariably overestimate the degree of stenosis and, for MRA and CTA, present a risk to the patient due to nephrotoxicity of the contrast agents used. An association can be drawn between CVD and renal arterial stenosis (RAS); approximately 90% of patients with RAS have also been diagnosed with atherosclerosis [5]. RAS is also a concern clinically due to its own morbidities of renal insufficiency, myocardial infarction, congestive heart failure, stroke, and death [6]. Due its high degree of sensitivity in the assessment of arterial stenosis, digital subtraction angiography (DSA) has been utilised as the "gold standard" for the diagnosis of RAS, however it carries a level of risk due to being an ionising and invasive technique and so is now only recommended for assessment of below-the-knee arterial disease and in cases where there is disagreement between non-invasive diagnostic techniques [2]. Consequently, there is clinical interest in improving the assessment capabilities of other non-invasive diagnostic modalities. Of these modalities, Doppler ultrasound

* Corresponding author at: Focas Research Institute, Technological University Dublin, Camden Row, Dublin 8, Ireland.
E-mail address: andrew.malone@tudublin.ie (A.J. Malone).

https://doi.org/10.1016/j.ejmp.2019.11.012
Received 1 July 2019; Received in revised form 31 October 2019; Accepted 15 November 2019
Available online 05 December 2019

Table 1
Compression testing Young's elastic modulus values given for various forms of PVA-c as compared to values of tissue *in vivo* (All values given in kPa).

Healthy vessel	Diseased vessel	Freeze thaw cycles	PVA-c (5% w/v)	PVA-c (10% w/v)		PVA-c (15% w/v)
24–83[¤]	116–751[¤]	1	2.5 ± 0.09[*]	24 ± 0.42[¶]	19 ± 2[†]	190[‡]
		2	2.7 ± 0.09[*]	70 ± 1.80[¶]	80 ± 16[†]	346[‡]
		3	3.5 ± 0.1[*]	87 ± 1.85[¶]	102 ± 12[†]	
		4	5.4 ± 0.12[*]	115 ± 6.63[¶]	136 ± 26[†]	
		5		135 ± 9.81[¶]	160 ± 42[†]	1840[‡]
		6			164 ± 34[†]	

[¤] Ref. [27–29].
[*] Ref. [23].
[¶] Ref. [24].
[†] Ref. [17].
[‡] Ref. [14].

presents as the least expensive option, in addition to being non-ionising and widely available. Clinical studies involving Doppler ultrasound have reported sensitivity of between 80% and 97% and specificity varying from 54% to 92% in the diagnosis of RAS [7–11], and hence further refinement of this technique is required.

In order to validate the efficacy of a new Doppler ultrasound analysis technique, a robust phantom testbed must first be developed; this allows for the technique to be assessed in a reliably consistent experimental environment designed to be anatomically realistic without the full complexities inherent with imaging *in vivo*. The purpose of this work was to develop a phantom design which could mimic one specific parameter of atherosclerosis, namely, vessel wall stiffening and allow for the validation of ultrasound techniques designed to measure or detect changes in wall stiffening. To date, many phantom designs have been used for assessment of Doppler ultrasound techniques. Law et al. conducted a comprehensive review of early flow phantom designs featuring internal tubing composed of materials such as glass, quartz, Teflon, and a number of polymers [12]. These materials have varying success at mimicking the acoustic behaviour of tissue *in vivo* as the materials can often cause unwanted distortion and attenuation of the ultrasound beam if not sufficiently acoustically analogous to human tissue. Consequently some researchers have attempted to reproduce realistic physical models of human vasculature through the use of excised vessels from human cadavers [13,14]. It has been shown, however, that excised arteries are susceptible to acoustic, mechanical, and geometric changes if not correctly stored and maintained [15]. It is also difficult to characterise excised vessels to allow for a high standard of acoustic and geometric reproducibility across phantoms. Additionally, the use of excised human tissue requires strict adherence to legislation and consideration of biological safety hazards that are not a concern when using non-biological materials. It is therefore desirable in the production of flow phantoms to use materials which can be well characterised and reproduced consistently to a high degree of acoustic and mechanical precision. One such material is polyvinyl alcohol cryogel (PVA-c).

PVA-c has been widely utilised as a component in the production of medical phantoms due to the fact that its mechanical properties can be controlled through physical and chemical cross-linking processes. The most common method used to initiate cross-linking is the application of sequential freeze-thaw cycles to aqueous PVA-c solutions [3,16–19]. PVA-c has been widely used as a tissue mimicking material (TMM) for ultrasound and MR imaging and its strength and robustness allow for its use in flow phantoms as a vessel mimicking material (VMM) [16,17,19–22].

The acoustic properties of tissue have been observed to change with the progression of arterial disease and have been well established in the literature. A comprehensive review of physical tissue properties over a large range of frequencies (1–100 MHz) is available in [23], which gives the speed of sound of healthy arteries in the range of 1560–1586 m s^{-1} with thinner arteries such as the renal artery having a speed of sound of 1565 m s^{-1}. Saijo et al. showed that, with the progression of disease in excised carotid arteries, the speed of sound in the intima varied from 1600 ± 20 m s^{-1} to 1680 ± 30 m s^{-1} [24]. Mechanical properties of arteries are more difficult to establish, however. The full elastic properties of a human artery vary significantly with respect to the layer of the vessel examined. The layer which is of most concern to the development of atherosclerosis is the innermost arterial layer, the intima, which consists of the basal lamina and the endothelial cells. The importance of this layer over other arterial layers is as this is where the formation of atherosclerotic plaque takes place [25]. McKee et al. showed that there are significant differences between measured Young's modulus values of human arteries in the literature, sometimes spanning several orders of magnitude [26]. More recently, Rezvani-Sharif et al. have shown that a typical healthy artery will have a Young's modulus of approximately 24.8–34.9 kPa from the internal elastic lamina [27]. Similarly, the values for diseased and fibrous arterial tissue has been reported to range from 182 to 649 kPa [28]. A systematic review of elasticity values reported in the literature was carried out by Boesen et al. [29]. They found that the Young's modulus varied from 39.7 to 83 kPa for healthy vessels, while disease vessels were found to have values in the region 116–751 kPa.

Table 1 presents data from several studies which investigated the mechanical properties of PVA-c, where reasonable approximations to vessel mechanical characteristics were obtained with relatively low concentrations of PVA-c [16,19,22,30]. One of the most important factors determining the degree of cross-linking in PVA-c is the rate at which the thaw takes place during free-thaw cycles [17,22]. This implies that sample volume is also an important factor in mechanical properties, as the thaw rate of a larger sample can be slowed due to the insulation provided to the inner volume by the larger external volume. Therefore, this raises the question as to whether using a relatively large compression test sample, such as those in ISO 7743 [31], is a valid comparison to the relatively small volumes of vessel mimicking samples. Another method of assessing the mechanical properties of viscoelastic materials is given in ISO 37 [32] which provides a procedure for tensile mechanical testing. The test object used for ISO 37 is dumbbell shaped and has both a closer cross-sectional area and surface area to typical vessel samples. This may allow for a more accurate estimation of the mechanical properties of the vessels.

The aim of the current work was to develop a robust phantom test bed capable of modelling the various stages of CVD utilising PVA-c as a vessel mimicking material. To this end, detailed acoustic and mechanical characterisation of the PVA-c formulations was performed, and the geometric reproducibility of phantom designs was assessed.

2. Materials and methods

2.1. Geometric fabrication

A 3D model of the renal artery based on CT scans of a healthy

Fig. 1. Photographs of some lumen moulds made using the low melting temperature alloy material.

volunteer, previously developed for use in constructing flow phantoms, was utilised in this work [20]. This model was used to produce a series of silicone inner lumen master moulds which featured a 7.6 mm lumen diameter and were constructed to allow the use of modular inserts to finely control the lumen diameter to simulate stenosis formation. The position along the vessel at which the stenosis was placed was selected in consultation with an experienced vascular technician. A low melting temperature alloy (LMA) with a melting point of 47 °C (MCP 47 Mining and Chemical Products Ltd., Northamptonshire, UK) was used with these inner lumen moulds to produce vessel lumen moulds. A series of larger outer vessel master moulds were constructed from the renal model featuring a diameter of 10.6 mm. By placing the LMA lumen mould inside the outer vessel mould, a negative space was left to form the vessel with a wall thickness of 1.5 mm. The larger outer vessel mould could be removed after the PVA-c had set, while the inner vessel mould could be removed by melting the LMA. Some representative examples of the LMA lumen moulds are shown in Fig. 1.

2.2. Tissue mimicking materials

2.2.1. PVA-c vessel mimic production

The components used in the production of the PVA-c VMM are outlined in Table 2. Two batches of PVA-c were made: a 10% w/v formulation and a 15% w/v formulation. The 15% w/v formulation differed only in the percentage of PVA-c (increased 5%) and deionised water (decreased 5%). The components used were selected to provide acoustic properties analogous to human arteries (approximately a speed of sound of 1565 m s^{-1} and an attenuation of 0.56 dB cm^{-1} MHz^{-1}). Two sizes of aluminium oxide particles were included to act as acoustic scatterers and provide speckle in the ultrasound images. An emulsion of silicone particles ranging in particle sizes 0.2–0.5 μm was used as an attenuator. Benzalkonium chloride was used as an anti-fungal agent to preserve the vessels, and glycerol was used as a plasticiser to fine tune the speed of the sound of the material.

Table 2
Constituent materials and concentrations used in the production of the 10% w/v PVA-c VMM.

Component	%(W/V)	Mass per 1L (g)
PVA	10.00	100.0
Aluminium oxide (0.3 μm)	0.73	7.3
Aluminium oxide (3 μm)	0.72	7.2
Silicone Emulsion	1.50	15.0
Benzalkonium chloride	0.46	4.6
Glycerol	5.00	50.0
Deionised water	81.59	815.9

The components were placed in a metallic beaker which was heated to 90 °C in a water bath and continually mixed. The temperature of the material was monitored and once it had reached 90 °C it was allowed to mix thoroughly at 100 revolutions per minute (rpm) for 1 h. The beaker was then removed from the water bath; the loss of water through evaporation was rectified by adding deionised water. The mixture was then placed in an ice bath and mixed continuously until it had cooled to 5 °C. The purpose of this cooling step was to ensure that the particles in the mixture remain in suspension when the material underwent its first freeze thaw cycle and to avoid sedimentation over a long freeze. Once the material was at 5 °C, it was injected via a 20 ml syringe into the interstitial space of the two-part vessel mould and the moulds were placed into the freezer. At the same time, a number of smaller cylindrical- and dumbbell-shaped samples were produced by pouring some of the batch directly into casting moulds which were also placed into the freezer. The cylindrical samples were in line with the procedure for producing compression test samples in ISO 7743 while the dumbbells corresponded to the tensile test samples from ISO 37. The dimensions of the cylindrical samples were 6 cm (diameter) and 1.5 cm (height), giving the cylinder a volume of 4.24×10^{-5} m^3 and a surface area of 8.48×10^{-3} m^2. The dumbbell samples featured two large flanges at each end to maximise friction between the sample and the jaws of the tensile tester, these flanges did not factor into the mechanical testing measurements and, therefore, their dimensions can be excluded. The remaining cuboid of the dumbbell samples had dimensions of 15 cm (length), 1 cm (width), and 5 mm (depth), giving it a volume of 7.5×10^{-6} m^3 and a surface area of 4.5×10^{-3} m^2. An important factor in material temperature change is the surface area to volume ratio (SA:V), a large SA:V indicates that a material will more rapidly approach a homogenous internal temperature uniform to its surroundings. The cylindrical samples had a SA:V of 200 m^{-1} while the dumbbell samples had a SA:V of 600 m^{-1}.

It is well established in the literature that the most important aspect of the freeze thaw cycle is the thawing section, specifically duration of the thawing section [33]. It was therefore important to ensure a consistent, homogeneous thaw for all samples. This was achieved by simply unplugging the freezer at the end of a freeze cycle to allow for a controlled thaw of all samples simultaneously. The internal temperature of the freezer could be continuously monitored by inserting a small flexible thermocouple probe which remained inside the freezer, with the door closed, until the thaw was completed. A single freeze thaw cycle lasted 40 h, consisting of a 16 h overnight freeze at −30 °C followed by a 24 h thaw to room temperature. Completed samples could be used immediately after freeze thaw cycling or stored in a 10% glycerol-water solution to prevent dehydration, a method which has been shown to be effective at maintaining the shelf life of PVA-c for up to 2 years [34].

2.2.2. Agar tissue mimic production

The tissue mimicking material was made in accordance with guidelines put forward by the IEC [35,36]. The production was carried out as specified by Ramnarine et al. [37].

2.2.3. Acoustic characterisation

An important step in ensuring that tissue mimicking materials are truly acoustically analogous to human tissue was characterising the acoustic properties of the materials, particularly speed of sound and attenuation. As mentioned previously, when VMM was produced, small cylindrical samples were made at the same time to allow for acoustic characterisation. Using these samples, acoustic characterisation was carried out using a scanning acoustic macroscope. The exact details of this system are given in more detail in previous work conducted by the group [20,22,34,38]. Briefly, this procedure consisted of using a scanning acoustic macroscope to determine the speed of sound and

attenuation of the cylindrical PVA-c samples through the use of a pulse echo substitution technique. A single element transducer was suspended over a water tank with a glass plate at the bottom acting as a plane reflector. Using a programme developed in LabVIEW (National Instruments, Austin, Texas, USA) the signal measured from the transducer could be recorded. By comparing the differences in signals between a sample and an unobstructed reference pulse, the speed of sound and attenuation can be determined. The acoustic characterisation was carried out at a frequency of 7.5 MHz.

2.2.4. Mechanical characterisation

During the production of the PVA-c VMM, a number of dumbbell shaped test samples were produced using a custom 3D printed mould. The purpose of these samples was to allow for tensile testing using a Lloyd Instruments LR30K*Plus* system (Ametek, USA). The samples were tested in accordance with ISO 37 [32]. The ISO defines tensile stress as the stress applied which causes elongation of the test sample in the direction of application of the stress, expressed as the force divided by the original cross-sectional area of the test sample. The tensile strain is defined as the elongation of the test sample in the direction of the tensile stress divided by the original length of the sample in that direction.

Sample preparation involved the conditioning of the test samples at the temperature of testing (18.5 ± 0.5 °C) for a minimum of 3 h prior to testing. The samples' width and depth were measured using a Vernier callipers before being fitted to the grips of the materials testing system. The system was then activated manually and the grips moved apart until a non-zero load was detected, indicating the samples were taut. Care was taken to ensure the samples were not experiencing a load greater than 0.5 N before zeroing the system at this position. The length of the sample between the two grips was measured and used to calculate the elongation setting. The system was then operated at a speed of 50 mm min^{-1} until a strain of 30% was reached, with the strain automatically released back to the zeroed position at a speed of 50 mm min^{-1} which consisted one tensile cycle. Each sample underwent 5 tensile cycles at 30% elongation with a 500 N load cell, producing 5 stress-strain curves. The analysis of these data was carried out in MATLAB (Mathworks, USA). The linear region of each stress-strain curve could be determined by performing second order numerical differentiation on the data and evaluating what region in the dataset had gone to zero. The Young's modulus was taken as the slope of the linear region of the 5th tensile cycle.

In order to ensure the validity of the mechanical testing results, a number of vessel-like test objects were also produced. These consisted of a standard hollow cylindrical shape but did not feature a bend like the vessel mimics so as to limit radial asymmetry. The cross-sectional area of these samples was calculated by measuring the inner and outer diameters and using the formula for the area of an annulus. The samples could then be fitted to the grips of the tensile testing system and tested using the same method as a dumbbell sample. As mentioned previously the cylindrical samples from ISO 7743 had a SA:V of 200 m^{-1} while the dumbbell samples from ISO 37 had a SA:V of 600 m^{-1}. It was assumed that the vessel-like samples could be considered as annular cylinders with dimensions of 5 cm (length), 10.6 mm (outer diameter), and 7.6 mm (inner diameter). The volume was 7.82×10^{-6} m^3 and the surface area was 5.5×10^{-3} m^2. This gave a SA:V of 707.06 m^{-1}. In principle, the true SA:V is likely lower as the freeze thaw cycles took place with the LMA insert in place, however due to the relatively high conductivity of metal compared to polymers, the effect of this piece could be neglected.

In total, 5 formulations of PVA-c were mechanically characterised, with 5 dumbbell samples and 6 vessel samples for each. The formulations tested were: 10% PVA-c 2, 3, 4, & 6 freeze thaw cycles and 15% PVA-c 2 freeze thaw cycles. The dumbbell and vessel samples were tested for correlation using a Pearson correlation analysis in MATLAB. The null hypothesis for the analysis was that the two variations of sample geometries were not correlated, the alternative hypothesis was that there was a correlation between the samples Young's modulus values with respect to the number of freeze thaw cycles. The null hypothesis was rejected if $p > 0.05$.

2.3. Geometric accuracy

In order to assess the reproducibility of fabrication method used to produce the phantom lumens, the geometric accuracy was determined. Five LMA lumen moulds were produced and the diameter was measured at three locations along the moulds. The locations measured were 10 mm from the inlet, 10 mm from the bend and 10 mm from the outlet. All measurements were made using a Vernier callipers and repeated three times. The diameters of the models were compared across the three locations and between models using a one-way analysis of variation (ANOVA) test. The five LMA moulds were then used to make 5 vessels which were implanted in phantoms at a depth of 7 cm, after undergoing 3 freeze thaw cycles each, and the LMA was removed. The phantoms were then connected to the flow system, filled with a 9.5% glycerol water solution which had a speed of sound of 1540 m s^{-1} and scanned in B-mode with an ultrasound system (Aixplorer, Supersonic Imagine, France) using a SL15-4 linear transducer at central transmission frequency of 5 MHz. Longitudinal images of the vessel were acquired for each specified diameter measurement location with the transducer positioned to place the focus of the transducer at the measurement location. The locations were specified using acoustic markers in the form of thread (diameter 1 mm) imbedded in the phantom perpendicularly to the vessel at the locations to be measured. These threads produced a strong reflected ultrasound signal allowing the locations to be found easily. For each measurement position three B-mode images were acquired.

The images were exported to MATLAB and analysed using a line profile tool. The line profile identified the intensity versus distance of a user specified region of interest which allowed for the clear differentiation of the vessel edges. An example of a line profile extracted from a B-mode image is shown in Fig. 2. The pixel distance of the vessel diameter was converted to mm by multiplying the pixel distance by the axial pixel size of the scanner. A one-way ANOVA test was carried out on the diameters in each phantom and between each phantom. The null hypothesis for this test was that there was no difference between any of the diameters measured. If $p < 0.05$ then the null hypothesis was rejected and the alternative hypothesis was that there was a statistical difference between the diameters. All statistical tests were carried out in MATLAB.

3. Results

3.1. Acoustic characterisation

The results of the acoustic characterisation are presented in Figs. 3 and 4. As the number of freeze thaw cycles was increased, a corresponding increase in speed of sound was found, varying in the range of 1556–1567 m s^{-1} for 2–6 f/t cycles. The values for the speed of sound were found to be within one standard deviation of the *in vivo* value for speed of sound of healthy renal arteries for all freeze thaw cycle values, with the exception of 2 freeze thaw cycles.

Similarly, the attenuation was found to increase with increasing numbers of freeze thaw cycles. The measured values of attenuation varied in the range 0.520–0.575 dB cm^{-1} MHz^{-1}. Again, these values were all within one standard deviation of the *in vivo* value of arterial attenuation for healthy renal arteries with the exception of 2 freeze thaw cycles.

3.2. Mechanical characterisation

The results of the mechanical characterisation are presented in

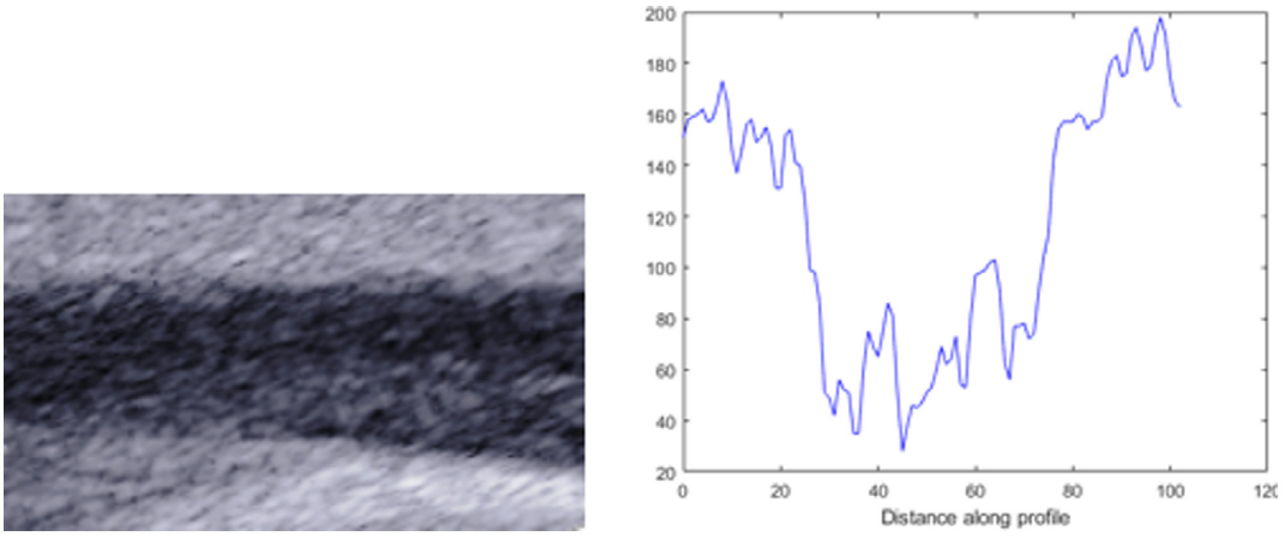

Fig. 2. An example B-mode image (left) of the phantom lumen and the line profile (right) extracted from it. The diameter of the vessel was calculated by multiplying the number of pixels across the lumen with the axial pixel size of the ultrasound scanner.

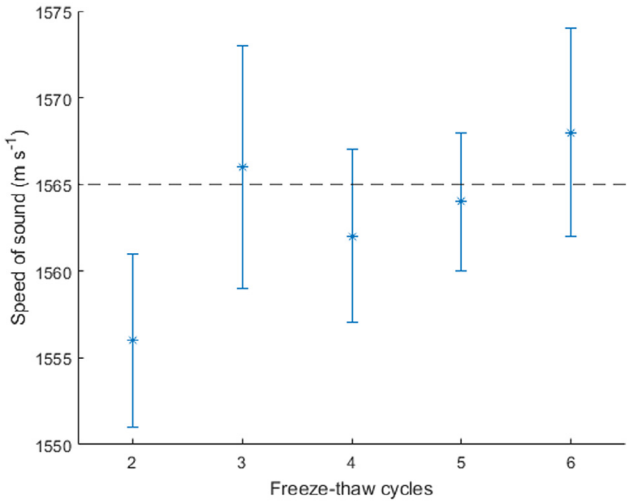

Fig. 3. The effect of increasing freeze thaw cycles on speed of sound measurements for PVA-c (10%). These measurements were made using a scanning acoustic macroscope at a frequency of 7.5 MHz. The dashed black line indicates the *in vivo* value for arterial speed of sound [23].

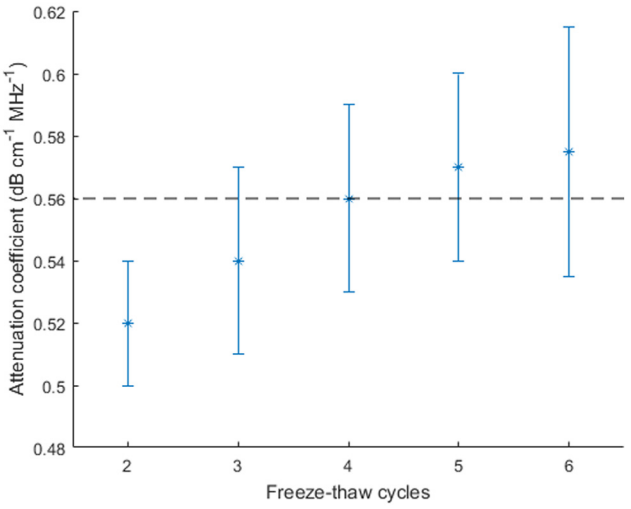

Fig. 4. The effect of increasing freeze thaw cycles on attenuation measurements for PVA-c (10%). These measurements were made using a scanning acoustic macroscope at a frequency of 7.5 MHz. The dashed black line indicates the *in vivo* value for arterial attenuation.

Fig. 5. For each number of freeze thaw cycle, the Young's moduli of the vessel-like samples were comparable to the Young's moduli values of the dumbbell test samples produced in accordance with ISO 37. The Young's modulus values with analysed using Pearson correlation, which gave an R^2 value of 0.9767. The p-value for this analysis was $p = 0.0013$, indicating that the R^2 value was highly significant and the alternative hypothesis was accepted.

3.3. Geometric accuracy

The measured mean diameter (in mm) of the 5 LMA cores at 3 measurement positions are presented in Table 3. A one-way ANOVA statistical test was carried out for the populations of diameters between the measurement locations and between the LMA cores. The p-value was $p = 0.3368$. Since $p > 0.05$, the null hypothesis was not rejected, indicating that the diameters were the same at each measurement location and for each LMA core. Table 3 also shows the diameters measured using the line profile analysis of the phantom lumens at the equivalent measurement locations after the LMA cores had been removed. Again, no significant difference in measured diameter was detected using the ANOVA test ($p = 0.1763$).

4. Discussion

A technique for producing a range of anatomically realistic renal artery flow phantoms featuring varying degree of vessel stiffening was developed. The procedure used in the production of the PVA-c material was outlined and a comprehensive mechanical and acoustic characterisation of PVA-c was carried out. The vessel mimics were implanted horizontally at a depth of 7 cm, analogous to the depth of the renal artery in the abdomen [39]. These flow phantoms displayed a range of stiffness values which modelled the progression of arterial disease allowing for the testing of diagnostic techniques for CVD.

To ensure that the materials used in the construction of these flow phantoms were an accurate facsimile of the tissues *in vivo*, the acoustic properties of the vessel mimicking material were evaluated using a scanning acoustic macroscope. The speed of sound of the material varied between 1556 and 1567 m s^{-1} and the attenuation varied

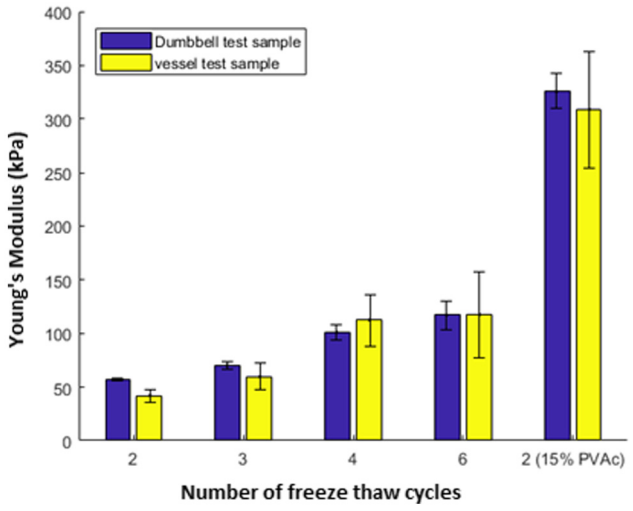

Fig. 5. Comparison of Young's modulus values for increasing freeze thaw cycles between ISO 37 dumbbell test samples and the vessel-like test sample.

Table 3
Comparison of mean diameters at three measurement locations across five LMA cores and five phantom lumens. LMA cores were measured using a callipers and the lumens were measured in B-mode.

Location	Mean Diameter LMA core [mm]	Mean Diameter phantom lumen [mm]
Inlet	7.61 ± 0.04	7.77 ± 0.04
Bend	7.58 ± 0.04	7.69 ± 0.05
Outlet	7.61 ± 0.04	7.66 ± 0.053

between 0.520 and 0.575 dB cm^{-1} MHz^{-1}. For 3–6 freeze thaw cycles, the values recorded were within one standard deviation of the *in vivo* value given in the literature for both the speed of sound and the attenuation of the material [23]. A general trend of increasing speed of sound and attenuation with respect to number of freeze thaw cycles was also observed. This trend has been seen previously in other studies [17,19]. The trend observed in this work is approximately linear, which is also similar to other studies, however there was an observed levelling off of the attenuation results as they reached large numbers of freeze thaw cycles. This result was believed to be indicative of the asymptotic limit of the PVA crosslinking being approached. Previous work by Fromageau et al. showed that as the number of freeze thaw cycles increases, the speed of sound, attenuation, and Young's modulus of PVA-c all follow a logarithmic profile of diminishing returns and that these samples of greater numbers of freeze thaw cycles had a higher degree of dehydration than other samples [40]. A possible explanation for this effect is that the PVA-c has approached a point of maximum polymerisation, above which additional polymer chains cannot form. If this is the case, then additional freeze thaw cycles above a certain threshold would provide less benefit than initial freeze thaw cycles to the point of redundancy. This threshold would most likely be proportional to the percentage of PVA used in the formulation as a larger percentage would have a larger number of monomers available for polymerisation and, therefore, a higher threshold.

The results of this study have indicated that increasing the speed of sound through mechanical means tends to also result in an increase in attenuation and Young's modulus as the PVA-c material undergoes further crosslinking. A potential alternative method to control the speed of sound of the material was suggested by Elvira et al. This method involved the addition of proplylene-glycol of different percentages to the water used in the production of the cryogel. This study observed a linear increase in speed of sound with respect to concentration of propylene-glycol with each additional 1% resulting in a corresponding increase in the speed of sound of the resulting material of $+5.46$ m s^{-1} [41]. This method allows for a fine control of the speed of sound without a corresponding increase in other acoustic or mechanical properties. When combined with the ability of components such as silicone emulsion to finely control the attenuation of the cryogel, this provides a potential production process whereby the material could be produced to have specific mechanical properties of density and Young's modulus and then the acoustic properties of speed of sound and attenuation could be adjusted to align more with the values *in vivo*.

Research into arterial acoustic properties in the later stages of arterial disease indicate a potential change in the properties of tissue; for example, Saijo et al. studied excised human coronary arteries featuring advanced atherosclerosis to determine their acoustic properties using a scanning acoustic macroscope [24]. The results showed that the intima showed significantly increased speed of sound values in regions with collagen fibre present and where the vessel had become calcified (1680 ± 30 m s^{-1} and 1810 ± 25 m s^{-1} respectively). This indicates that as CVD progresses a more thorough modelling of the situation *in vivo* would include a corresponding increase in speed of sound. Decoupling of Young's modulus from speed of sound to allow independent control of each variable may prove difficult, however. Additional research into PVA-c formulations with higher speed of sound values is needed.

To ensure that the phantoms were accurately modelling the progression of CVD, the mechanical properties of the PVA-c material were measured for a number of freeze thaw cycles. Some previous mechanical characterisation of PVA-c has relied on the use of compression testing as outlined in ISO 7743, working under the assumption that a large cylindrical test sample would have broadly equivalent mechanical properties to the much smaller vessel [16,19,22,30,42]. As discussed earlier there are a number of limitations to this assumption, and a more direct comparison of mechanical properties was investigated using tensile testing, as outlined in ISO 37. The tensile testing was carried out using a dumbbell-shaped sample and compared directly to the vessel using a hollow cylindrical vessel-like test sample. It was believed that this would allow for a more direct comparison because the elastic properties of PVA-c are strongly related to the rate of thawing, which will take place over a longer timescale for a sample with a low SA:V. The SA:V of the cylindrical samples was 200 m^{-1} while the dumbbell samples had a SA:V of 600 m^{-1}. When compared to the vessel samples, which had a SA:V of 707.06 m^{-1}, the SA:V of both samples were low. However, the dumbbell test samples were much closer to the value calculated for the vessels. The Young's modulus values for the dumbbell samples varied in the range 62–119 kPa for the 10% w/v PVA-c material for 2–6 freeze thaw cycles, and a single 15% w/v PVA-c batch was found to have a Young's modulus of 320 kPa for 2 freeze thaw cycles.

One parameter which was not assessed in this study which is potentially of interest was the density of the PVA-c material and how it responded to successive freeze thaw cycles. Fromageau et al. examined the relationship between density and freeze thaw cycles for 10% PVA-c. The density measurements were made using Archimedes' principle by producing a range of water glycerol solutions of known density between 1035 kg m^{-3} and 1060 kg m^{-3} and placing each sample to be tested in each solution until it was found to float in a mid-equilibrium position. The results of this analysis showed that, similar to speed of sound measurements, the density of the PVA-c material followed an approximate logarithmic relationship with a stabilisation of density values above approximately 6 freeze thaw cycles [40]. This result is in line with expectations based on the current understanding of the PVA-c crosslinking mechanism. It is likely that, similar to speed of sound, the density increase of PVA-c is related to the formation of additional polymer structure in the material and the availability of monomers in solution to undergo polymerisation. As such, it would be expected that, similar to speed of sound and Young's modulus, the density of the material would rise significantly for formulations with higher concentrations of PVA.

For each freeze thaw cycle, the vessel-like sample showed very similar results to the dumbbell sample. The two sample types were shown to be correlated (R^2 = 0.9767). This indicated that the dumbbell samples were extremely accurate in their modelling of the true stiffness values of the vessels produced for the phantoms. This further indicates that tensile testing carried out in accordance with ISO 37 is a more useful quantitative tool for the mechanical characterisation of PVA-c is. It is worth noting, however, that as the number of freeze thaw cycles increases, a stiffness maximum will gradually be achieved. This can be seen in Fig. 5 where the increase in Young's modulus is less as the number of freeze thaw cycles increases. This would indicate that if the number of freeze thaw cycles is sufficiently large, the difference in rate of thawing due to sample volume becomes less significant as the material approaches its stiffness maximum regardless.

The Young's modulus values measured closely followed the literature values for approximate tissue stiffness. The most recent literature regarding vessel stiffness estimated a high end for healthy arterial stiffness of 34.9–83 kPa [27,29] and an estimated range of diseased vessel stiffness of 116–751 kPa [28,29]. This indicates that for the samples produced, the 10% w/v PVA-c demonstrated an ideal healthy vessel stiffness for 2–3 freeze thaw cycles while the low end of typical diseased vessel stiffness was achieved for 4–6 freeze thaw cycles. There is a limit to the achievable vessel stiffness for a given percentage of PVA-c which, in addition to the inconvenience of the relatively long production times, preclude the use of 10% w/v PVA-c from suitably mimicking the higher stiffnesses recorded in diseased arteries. For this, 15% w/v PVA-c can be used at as low as 2 freeze thaw cycles to mimic the more developed stages of the disease. In order to mimic an advanced form of atherosclerosis, the 15% w/v PVA-c solution could be tested for suitability as a vessel mimic at higher freeze thaw cycles, although the value is well within its range of possible stiffnesses as 15% w/v PVA-c has been observed with Young's modulus values as high as 1840 kPa [16]. The 15% w/v PVA-c solution would need to be acoustically characterised to ensure its speed of sound and attenuation would remain within limits, however. The observed trend of linearly increasing speed of sound and attenuation in this study indicated that as the polymer crosslinking takes place, these acoustic parameters increase, therefore it would be expected that, as a 15% w/v PVA-c solution would have more monomers available in solution for crosslinking, the speed of sound and attenuation would be dramatically increased. In this case, the formulation could be adapted to contain lower concentrations of glycerol and silicone emulsion. The concentration of the aluminium oxides could also be lowered to reduce attenuation further at the expense of the "speckle" they provide when scanned in B-mode.

Finally, the two populations of diameter measurements were compared using a one-way ANOVA statistical test, first on the LMA core population between the three measurement locations and second as a comparison between the LMA core diameters and the phantom lumen diameters. The tests failed to reject the null hypothesis for both tests (p = 0.3368, p = 0.1763). This indicated that firstly, the fabrication of the LMA cores was sufficiently reproducible to reliably result in the same diameter for the LMA cores; and, secondly, that the LMA cores resulted in consistent phantom lumen diameters.

5. Conclusion

A method was developed to produce a series of robust flow phantoms to model CVD. The material PVA-c was demonstrated to be a useful tool in the mimicking of arteries, specifically the renal artery in this case. PVA-c is particularly useful in the precise control over its final mechanical properties afforded to the manufacturer. This work has shown that PVA-c can be produced in artery-specific geometries with accurate and reproducible acoustic properties. In addition, the mechanical properties of complex vessel geometries can be accurately determined using tensile testing and the dumbbell test sample geometry outlined in ISO 37. Finally, the fabrication process of the vessel mimicking material can be carried out to achieve accurate and reproducible phantom lumen diameters.

PVA-c represents a useful material for the modelling of CVD in phantoms repetition, allowing for more powerful research into the development and progression of arterial disease in the form of the fluid dynamic behaviour with respect to vessel stiffness. This is potentially of great clinical importance due to the fact that CVD represents the single greatest cause of mortality in patients. Therefore, the ability to precisely model the progression of this disease in a reproducible phantom testbed allows for the examination of new quantitative assessment techniques to increase the efficacy of diagnostic screening for CVD.

Acknowledgments

The authors would like to acknowledge the Dean of Graduate Fiosraigh Research Programme, awarded by the Dublin Institute of Technology (now Technological University of Dublin), and the Young Investigator Grant awarded by the Irish Association of Physicists in Medicine, for their funding of this work. Also, the authors would like to thank the FOCAS research institute and School of Mechanical and Design Engineering of TU Dublin for access to core equipment facilities. In particular we would like to thank Neil Branigan for his assistance with the use of the LR30KPlus material testing system.

References

[1] World Health Organisation. Cardiovascular diseases (CVDs). https://www.who.int/en/news-room/fact-sheets/detail/cardiovascular-diseases-(cvds); 2017 [accessed May 16, 2019].
[2] Aboyans V, Ricco J-B, Bartelink M-LEL, Björck M, Brodmann M, Cohnert T, et al. ESC guidelines on the diagnosis and treatment of peripheral arterial diseases, in collaboration with the European society for vascular surgery (ESVS). Eur J Vasc Endovasc Surg 2017;2017(39):763–816. https://doi.org/10.1016/J.EJVS.2017.07.018.
[3] Brusseau E, Fromageau J, Finet G, Delachartre P, Vray D. Axial strain imaging of intravascular data: results on polyvinyl alcohol cryogel phantoms and carotid artery. Ultrasound Med Biol 2001;27:1631–42. https://doi.org/10.1016/S0301-5629(01)00451-3.
[4] Zaman A, Helft G, Worthley S, Badimon J. The role of plaque rupture and thrombosis in coronary artery disease. Atherosclerosis 2000;149:251–66. https://doi.org/10.1016/S0021-9150(99)00479-7.
[5] Plouin P-F, Bax L. Diagnosis and treatment of renal artery stenosis. Nat Rev Nephrol 2010;6:151–9. https://doi.org/10.1038/nrneph.2009.230.
[6] Browne JE, King D, Fagan AJ, Chari D, Moran CM. An investigation of the detection capability of pulsed wave duplex Doppler of low grade stenosis using ultrasound contrast agent microbubbles – an in-vitro study. Ultrasonics 2019;96:48–54. https://doi.org/10.1016/j.ultras.2019.04.003.
[7] Eklöf H, Ahlström H, Magnusson A, Andersson L-G, Andrén B, Hägg A, et al. A prospective comparison of duplex ultrasonography, captopril renography, MRA, and CTA in assessing renal artery stenosis. Acta Radiol 2006;47:764–74. https://doi.org/10.1080/02841850600849092.
[8] Soares GM, Murphy TP, Singha MS, Parada A, Jaff M. Renal artery duplex ultrasonography as a screening and surveillance tool to detect renal artery stenosis. J Ultrasound Med 2006;25:293–8. https://doi.org/10.7863/jum.2006.25.3.293.
[9] Williams GJ, Macaskill P, Chan SF, Karplus TE, Yung W, Hodson EM, et al. Comparative accuracy of renal duplex sonographic parameters in the diagnosis of renal artery stenosis: paired and unpaired analysis. Am J Roentgenol 2007;188:798–811. https://doi.org/10.2214/AJR.06.0355.
[10] Browne JE, Watson AJ, Hoskins PR, Elliott AT. Validation of a sensitivity performance index test protocol and evaluation of colour Doppler sensitivity for a range of ultrasound scanners. Ultrasound Med Biol 2004;30:1475–83. https://doi.org/10.1016/j.ultrasmedbio.2004.09.005.
[11] King DM, Moran CM, Browne JE. Comparative review of imaging methods used for diagnosing renal artery stenosis. Ultrasound 2012;20:135–41. https://doi.org/10.1258/ult.2012.011037.
[12] Law YF, Johnston KW, Routh HF, Cobbold RSC. On the design and evaluation of a steady flow model for Doppler ultrasound studies. Ultrasound Med Biol 1989;15:505–16. https://doi.org/10.1016/0301-5629(89)90103-8.
[13] Dabrowski W, Dunmore-Buyze J, Rankin RN, Holdsworth DW, Fenster A. A real vessel phantom for imaging experimentation. Med Phys 1997;24:687–93. https://doi.org/10.1118/1.597991.
[14] Dabrowski W, Dunmore-Buyze J, Cardinal HN, Fenster A. A real vessel phantom for flow imaging: 3-D Doppler ultrasound of steady flow. Ultrasound Med Biol 2001;27:135–41. https://doi.org/10.1016/S0301-5629(00)00277-5.
[15] Wilhjelm JE, Vogt K, Jespersen SK, Sillesen H. Influence of tissue preservation methods on arterial geometry and echogenicity. Ultrasound Med Biol 1997;23:1071–82. https://doi.org/10.1016/S0301-5629(97)00034-3.
[16] Chu KC, Rutt BK. Polyvinyl alcohol cryogel: an ideal phantom material for MR

studies of arterial flow and elasticity. Magn Reson Med 1997;37:314–9. https://doi.org/10.1002/mrm.1910370230.
[17] Surry KJM, Austin HJB, Fenster A, Peters TM. Poly(vinyl alcohol) cryogel phantoms for use in ultrasound and MR imaging. Phys Med Biol 2004;49:5529–46. https://doi.org/10.1088/0031-9155/49/24/009.
[18] Pazos V, Mongrain R, Tardif JC. Polyvinyl alcohol cryogel: optimizing the parameters of cryogenic treatment using hyperelastic models. J Mech Behav Biomed Mater 2009;2:542–9. https://doi.org/10.1016/J.JMBBM.2009.01.003.
[19] King DM, Moran CM, McNamara JD, Fagan AJ, Browne JE. Development of a vessel-mimicking material for use in anatomically realistic Doppler flow phantoms. Ultrasound Med Biol 2011;37:813–26. https://doi.org/10.1016/j.ultrasmedbio.2011.02.012.
[20] King DM, Ring M, Moran CM, Browne JE. Development of a range of anatomically realistic renal artery flow phantoms. Ultrasound Med Biol 2010;36:1135–44. https://doi.org/10.1016/j.ultrasmedbio.2010.04.017.
[21] King DM, Fagan AJ, Moran CM, Browne JE. Comparative imaging study in ultrasound, MRI, CT, and DSA using a multimodality renal artery phantom; Comparative imaging study in ultrasound, MRI, CT, and DSA using a multimodality renal artery phantom. Med Phys 2011;38:565–73. https://doi.org/10.1118/1.3533674.
[22] Cournane S, Cannon L, Browne JE, Fagan AJ. Assessment of the accuracy of an ultrasound elastography liver scanning system using a PVA-cryogel phantom with optimal acoustic and mechanical properties. Phys Med Biol 2010;55:5965–83. https://doi.org/10.1088/0031-9155/55/19/022.
[23] Duck FA. Chapter 4 – Acoustic properties of tissue at ultrasonic frequencies. In Phys. Prop. Tissues; 1990, p. 73–135. doi: 10.1016/B978-0-12-222800-1.50008-5.
[24] Saijo Y, Filho E, Sasaki H, Yambe T, Tanaka M, Hozumi N, et al. Ultrasonic tissue characterization of atherosclerosis by a speed-of-sound microscanning system. IEEE Trans Ultrason Ferroelectr Freq Control 2007;54:1571–7. https://doi.org/10.1109/TUFFC.2007.427.
[25] Stary HC, Blankenhorn DH, Chandler A, Bleakley, Glagov S, Insull W, Richardson M, et al. AHA medical/scientific statement special report a definition of the intima of human arteries and of its atherosclerosis-prone regions a report from the committee on vascular lesions of the council on arteriosclerosis, American Heart Association. Circulation 1992;85:391–405.
[26] McKee CT, Last JA, Russell P, Murphy CJ. Indentation versus tensile measurements of Young's modulus for soft biological tissues. Tissue Eng Part B Rev 2011;17:155–64. https://doi.org/10.1089/ten.TEB.2010.0520.
[27] Rezvani-Sharif A, Tafazzoli-Shadpour M, Avolio A. Progressive changes of elastic moduli of arterial wall and atherosclerotic plaque components during plaque development in human coronary arteries. Med Biol Eng Comput 2019;57:731–40. https://doi.org/10.1007/s11517-018-1910-4.
[28] Poree J, Chayer B, Soulez G, Ohayon J, Cloutier G. Noninvasive vascular modulography method for imaging the local elasticity of atherosclerotic plaques: simulation and in vitro vessel phantom study. IEEE Trans Ultrason Ferroelectr Freq Control 2017;64:1805–17. https://doi.org/10.1109/TUFFC.2017.2757763.
[29] Boesen ME, Singh D, Menon BK, Frayne R. A systematic literature review of the effect of carotid atherosclerosis on local vessel stiffness and elasticity. Atherosclerosis 2015. https://doi.org/10.1016/j.atherosclerosis.2015.09.008.
[30] Duboeuf F, Liebgott H, Basarab A, Brusseau E, Delachartre P, Vray D. Static mechanical assessment of elastic Young's modulus of tissue mimicking materials used for medical imaging. In 2007 29th Annu. Int. Conf. IEEE Eng. Med. Biol. Soc., IEEE; 2007, p. 3450–3. doi: 10.1109/IEMBS.2007.4353073.
[31] International Organization for Standardisation. ISO 7743:2011 rubber, vulcanized or thermoplastic – determination of compression stress-strain properties; 2011.
[32] International Organization for Standardisation. ISO 37:2017 rubber, vulcanized or thermoplastic – determination of tensile stress-strain properties; 2017.
[33] Baker MI, Walsh SP, Schwartz Z, Boyan BD. A review of polyvinyl alcohol and its uses in cartilage and orthopedic applications. J Biomed Mater Res Part B Appl Biomater 2012;100B:1451–7. https://doi.org/10.1002/jbm.b.32694.
[34] King D. Development of renal phantoms for the evaluation of current and emerging ultrasound technology Dublin Institute of Technology; 2009. https://doi.org/10.21427/D7VP4C.
[35] Teirlinck CJPM, Bezemer RA, Kollmann C, Lubbers J, Hoskins PR, Fish P, et al. Development of an example flow test object and comparison of five of these test objects, constructed in various laboratories. Ultrasonics 1998;36:653–60. https://doi.org/10.1016/S0041-624X(97)00150-9.
[36] International Electrotechnical Commission. Ultrasonics – flow measurement systems – flow test object; 2001.
[37] Ramnarine KV, Anderson T, Hoskins PR. Construction and geometric stability of physiological flow rate wall-less stenosis phantoms. Ultrasound Med Biol 2001;27:245–50. https://doi.org/10.1016/S0301-5629(00)00304-5.
[38] Browne JE, Ramnarine KV, Watson AJ, Hoskins PR. Assessment of the acoustic properties of common tissue-mimicking test phantoms. Ultrasound Med Biol 2003;29:1053–60. https://doi.org/10.1016/S0301-5629(03)00053-X.
[39] Ostrowski ST, Tothill P. Kidney depth measurements using a double isotope technique. Br J Radiol 1975;48:291–4. https://doi.org/10.1259/0007-1285-48-568-291.
[40] Fromageau J, Gennisson J-L, Schmitt C, Maurice RL, Mongrain R, Cloutier G. Estimation of polyvinyl alcohol cryogel mechanical properties with four ultrasound elastography methods and comparison with gold standard testings. IEEE Trans Ultrason Ferroelectr Freq Control 2007;54:498–509. https://doi.org/10.1109/TUFFC.2007.273.
[41] Elvira L, Durán C, Higuti RT, Tiago MM, Ibáñez A, Parrilla M, et al. Development and characterization of medical phantoms for ultrasound imaging based on customizable and mouldable polyvinyl alcohol cryogel-based materials and 3-D printing: application to high-frequency cranial ultrasonography in infants. Ultrasound Med Biol 2019;45:2226–41. https://doi.org/10.1016/J.ULTRASMEDBIO.2019.04.030.
[42] Kawasaki T, Sasayama S, Yagi S-I, Asakawa T, Hirai T. Non-invasive assessment of the age related changes in stiffness of major branches of the human arteries. Cardiovasc Res 1987;21:678–87. https://doi.org/10.1093/cvr/21.9.678.